

# Link Lifetimes: Distribution, Estimation and Application in Mobile Ad hoc Networks

Sridhar K. N.

*Institute for Infocomm Research  
21, Heng Mui Keng Terrace, Singapore 119613*

Mun Choon Chan

*School of Computing  
National University of Singapore, Singapore 117543*

---

## Abstract

Lifetime of a link defines the amount of time the link is available for transmission. In this work, we begin with associating a statistical parametric model for link lifetime distribution for commonly used mobility patterns. The study reveals interesting properties about link lifetimes, including findings showing that lifetimes of the mobility patterns studied are of *wear-out* type, rather than random failure. Next, we propose a heuristics based link lifetime estimation process that exploits knowledge of the associated mobility pattern and show that the estimation performs well under diverse operating conditions. Finally, we present an application of link lifetime. In this application, link lifetime is used as an indicator of end-to-end channel-quality to carry out packet scheduling decisions.

*Key words:* Link Lifetimes, statistical parametric models, estimation, packet-scheduling.

---

## 1 Introduction

A Mobile Ad Hoc Network (MANET) is a wireless network consisting of mobile nodes, which can communicate with each other without any infrastructure (base-stations) support. The nodes are free to move randomly and organize themselves arbitrarily. Every node communicates via wireless radios that have limited transmission capabilities. Due to this constraint on transmission, not all nodes are within the transmission range of each other. If a node wishes to communicate with a node outside its transmission range, it needs the help

of other nodes in constructing a multihop route. A key challenge in MANET is that communication has to be carried out with changing network topology due to node mobility.

The goal of this work is to have a detailed study of the link lifetime characteristics associated with commonly used mobility patterns. Such understanding is helpful in exploring different ways in which link lifetimes can be used across various networking layers. In this regard, we begin with collecting link lifetimes over diverse mobility patterns, and associating a statistical parametric model for link lifetime distribution. This study reveals interesting properties about link lifetimes, including findings showing that lifetimes of the mobility patterns studied are of *wear-out* type, where lifetimes are dependent on the current age. Random failure, a common assumption in many existing works, does not fit any one of the mobile patterns studied. Next, we propose a link lifetime estimation heuristic that exploits knowledge of the statistical property of associated mobility pattern. This estimation process provides higher accuracy and requires fewer samples than a histogram based method.

Finally, we present an application of link lifetimes. In the application, residual link lifetime is used to indicate end-to-end channel quality, in order to provide “channel-awareness” to packet scheduling mechanism. A packet scheduling mechanism, *CaSMA*, uses link lifetime as a channel-quality indicator. We provide detailed description of *CaSMA*, including performance comparison with similar packet scheduling schemes.

The paper is organized as follows. Section 2 describes the related works on link durations. Section 3 focuses on the study of link lifetime, in which a parametric statistical model is associated to the lifetime distribution of various mobility models. Section 4 describes the link lifetime estimation process and its performance evaluation. Section 5 describes the application of link lifetime estimation in channel-aware packet scheduling. The paper is summarized and concluded in Section 6.

## 2 Related Work

In majority of the earlier works [1–5], Link Change Rate (LCR) and Link Duration (LD) metrics are used to infer link quality. The LCR [1] metric is defined as the number of communication links forming and breaking between nodes over a given time  $T$ . The LD metric describes the lifetime of communication links. Cho et al., [3] show that LCR is not suitable as a metric for link lifetime estimation as its relation with the route lifespan depends on the node density, which may not be uniform in many mobility models. The conclusion that LD is a good unified mobility metric based on constant velocity (CV)

model. This conclusion is mainly because of relation between LD and route lifespan, which they say is invariant of the mobility model used.

Lenders et al., [4] analyze the impact of human mobility on the link and route lifetime of mobile ad hoc networks. They analyze the data gathered from a real ad hoc network of 20 PDAs connected via 802.11b wireless interfaces. They found that interruptions due to human mobility and collisions/interference have a completely different impact on the lifetime of links and routes. Authors also compared the empirical link lifetime with those obtained by statistical mobility models. The results show that the distribution of the random waypoint and the random reference point group mobility models are close to the empirical distribution.

One of the first studies concerning the analysis of path duration was by Bai et al., [2]. Based on experimental results obtained by simulations, they assume that the lifetime of a path with four or more hops can be approximated by an exponential distribution. However, the authors do not consider the fit of any other standard distribution. Moreover, they do not justify the selection of an exponential distribution with any mathematical validation. To cope with this shortcoming, Han et al., [6] basing their work on Palms theorem, state that, under certain circumstances, the lifetime associated to those paths with a large number of hops converges to an exponential distribution. The previous works present a clear disadvantage as they provide a solution for the analysis of paths which is valid only for routes with a large number of hops. Therefore their study could not be fully applied to many ad hoc networks and practical MANET applications where the paths only consist of 1 to 4 hops. The popularity of the exponential fitting has made it a common approximation in other works like [7]. Most authors have analyzed path duration by means of empirical results. For instance, [3] have shown that the mean residual lifetime of routes depends on the number of hops as well as on the mean link duration. On the other hand, [8] analytically proves that the average lifetime of a path decreases with its length. An analytical study on this aspect is carried out by Tseng et al. They based the analysis of the route lifetime on a spatial discrete model [9]. This study simplifies a MANET into a cellular network composed of hexagonal cells to compute the path availability. In [10], authors formally describe the distribution function of path duration assuming that nodes move according to a CV model.

The work by Gerharz et al. [11] on link duration in mobile wireless ad hoc network is closest to our work. They found that link durations vary with age and proposed techniques to measure residual lifetime online. They then proceed to propose two metrics for selecting a stable link: highest average residual lifetime and highest 75% quantile. From their analysis they found that initially a link's average residual lifetime decreases with increasing current age, and after a threshold, where threshold corresponds to the modal value

of link duration distribution, the residual lifetime increases with current age. However, in our simulations we found that this may not be true in some cases.

Cheng et al., [12] also study the distribution of link lifetimes in ad hoc network. However, they focus mainly on the factors which influence link lifetime. They consider the number of mobile nodes, node minimum speed and moving probability as dominating factors that influence link lifetime. From our experiments, we observe that average node density does not differ much across different mobility models. In [12], the authors also mention the possibility of considering route length along with route lifetimes though no algorithm was proposed.

Yih-Chun Hu et al., [13] explore the cache strategies in DSR and propose some mobility metrics. They found that link-cache strategies are better than path-cache strategies. As one of the link-cache strategy, they propose technique to combine stability value of a link, which is dependent on the usage of the link, and hop-count. They found that this technique though performs better, not better than a static scheme of 5 seconds expiration. We will show that our scheme performed better than the best link-cache schemes.

### 3 Study of Link Lifetime

In our work, we define link lifetime as follows. Consider a node  $n_1$ , with transmission range  $T$ . Let node  $n_2$  comes within the transmission range of  $n_1$  at time  $t_1$ . We call this time  $t_1$  the *link initiation time*. Now, let us consider, at some point of time in future  $t_2$  ( $t_2 > t_1$ ), the node  $n_2$  moves out of transmission range of  $n_1$ . Then the time  $t_2$  is termed as link termination time. *Link lifetime is the difference between the link initiation time and link termination time* ( $t_2 - t_1$ ).

An implicit assumption in our work is that distance is the dominant factor in determining the link quality. While we know the perfect disk communication model is not true in practice, we believe that using distance as the key parameter to determine transmission range is sufficient to provide useful insight into the statistical properties of link lifetimes.

#### 3.1 Overall Approach

The approach we have taken is based on the techniques used in the field of reliability engineering. In reliability studies, engineers study the probability that a system (vehicle, machine, device) will perform its function for a spec-

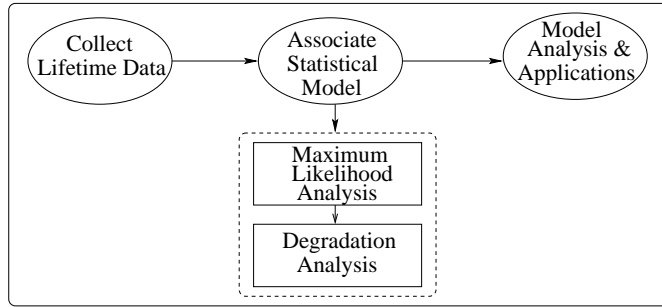


Fig. 1. Link lifetime study process

ified period [14]. The study considers the lifetime of the entity and various parameters that affect this lifetime. We believe that a link between two nodes can be one such entity, and we can adopt similar techniques.

Our approach is depicted in Figure 1, and has three steps, namely: (1) collection of lifetime data (2) association of statistical model and (3) analysis of model.

A statistical study on entity lifetime begins with collecting failure-time data (link lifetime data). Along with failure data, degradation data is also collected whenever it is available. Assume that a link “fails” when the two associated nodes move too far away from each other, degradation data in our context refers to how the distance between the two nodes varies. This is presented in Section 3.2.

The next step in the process is to associate a parametric statistical model to describe a set of data or a process that generates the set of data. A statistical model serves a number of purposes [14], including studying system stability and making estimations (lifetime durations), comparing different environments under which, the entities operate and checking the veracity of the performance claims.

Typical procedure in associating the statistical model involves two steps. First step uses the failure data and maximum likelihood (ML) approach, whereas, the second step uses the degradation data and carries out degradation analysis. The maximum likelihood method is the most popular method used for fitting statistical models to data. It has been shown that [15], under regular conditions, ML estimators are optimal when the samples are large. From the point of view of statistical studies, ML estimation and degradation analysis can be categorized as enumerative study and analytic study, respectively. Typically, enumerative study begins by collecting and carefully evaluating the samples, and further making an inference about the population from which the samples were collected. On the other hand, analytic study answers questions about processes that generate samples over time. Together, they enhance the accuracy of lifetime distribution model estimation. The details for association

of statistical model is presented in Sections 3.3 and 3.4.

Once a statistical model is associated with the lifetime, including the degradation data analysis, we perform the final step. In this step, we evaluate the accuracy of the associated statistical model by assuming that the associated model is correct, and look at how well the generated hazard function matches the measured data. This is presented in Section 3.5.

### *3.2 Collection of Lifetime Data - Lifetime Duration Distribution*

#### *3.2.1 Mobility Patterns*

There have been various mobility models or patterns proposed for MANETs. These patterns try to capture most of the common mobility patterns, but few patterns capture realistic movements of nodes in MANETs.

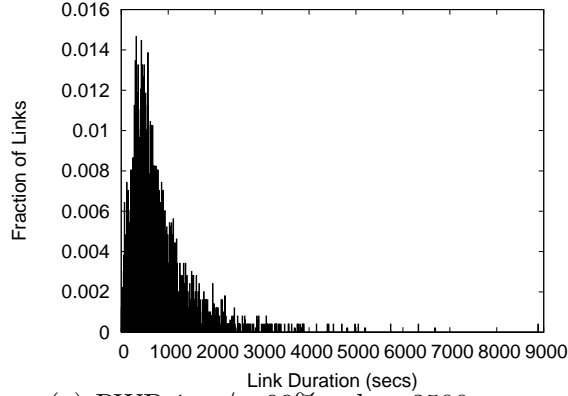
In our work, we use the following mobility patterns: random waypoint (RWP), Reference Point Group Mobility (RPGM), Manhattan mobility model [16] and a scenario based campus mobility model.

The first three mobility models are popular but generic models, and are chosen based on the recommendations of the IMPORTANT framework [2]. The IMPORTANT framework defines protocol independent metrics such as the average degree of spatial dependence, average degree of temporal dependence, average relative speed and geographic restrictions to capture the mobility characteristics. It also argues that the mobility models chosen (for simulation studies in MANETs) should span all the mobility characteristics described in the framework. Further, authors also show that the set of mobility models we have chosen satisfy these characteristics.

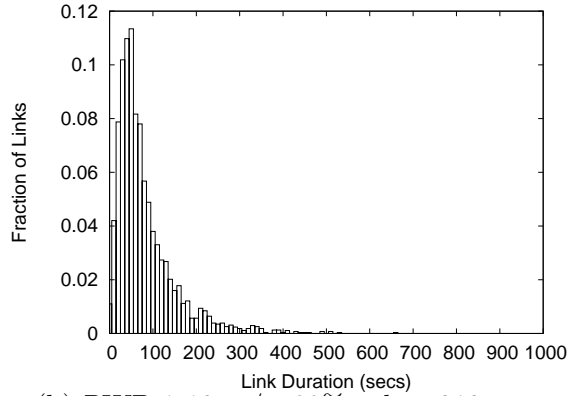
However, the above mobility patterns are still generic models. In order to evaluate a more realistic mobility pattern, we include a fourth mobility model that models movement in small campus environments, generated by the EGRESS tool [17, 18]. EGRESS models signal degradation due to obstacles in an environment with buildings, and allows different movement patterns for different user types. The node mobility also includes mobility inside buildings. The model is scenario based as the building structures, obstacle types and user behaviors have to be pre-defined for a specific scenario.

#### *3.2.2 Simulation Environment and Data Collection*

We use different generators for different mobility patterns. In addition, a single mobility pattern is generated using three different tools so that when we draw



(a) RWP 1 m/s, 99% value: 3500 secs



(b) RWP 1-10 m/s, 99% value: 310 secs

Fig. 2. Random waypoint lifetime distributions

a conclusion, the probability of the conclusion being correct is higher. We use the “setdest” tool, which comes with the distribution of NS-2 [19], mobility generator obtained from the Toilers group [20] and the tool from the bonnmotion group [21] to generate random waypoint mobility pattern. Similarly, mobility generator obtained from the Toilers group [20], the tool from the Nile group at USC [22] and the tool from the bonnmotion [21] group is used to generate the group mobility (RPGM) patterns. For Manhattan mobility patterns, the generators from the Nile group at USC [22] and the bonnmotion [21], respectively, are used. For the group mobility models, we consider three cases. In the first case, termed as RPGM1, we have a single group with 50 nodes. In the second case, termed as RPGM2, we consider 5 groups with 10 nodes each. Finally, in RPGM3, there are 10 groups with 5 nodes each.

For the campus mobility model, we use the EGRESS tool provided by the authors. The topology generated has 9 buildings (3 office buildings, 5 lecture theaters and 1 cafeteria). The buildings are connected by various pathways and junction points. Each building type has multiple floors (except cafeteria, which has single floor), with same layout on all the floors, and a different floor layout for different type of buildings. Two mobility speeds are considered,

walking (0 - 1m/s) and driving (0-10 m/s). The speeds are chosen based on the context (type of the node and the position of the node).

In each simulation, there are 50 nodes, with each node having a transmission range of 250 m. The simulation area is 1000 m x 1000 m. For Manhattan, there are 4 vertical and 4 horizontal roads. Each road has 2 lanes. So a single block would be of size 200 m x 200 m. The simulation duration is 1000 secs. To remove the effects due to congestion, there is no data traffic among the nodes. Therefore, link breaks are predominantly due to the mobility. For the study of link durations and residual lifetimes in RWP, RPGM and Manhattan, only the speeds of 1 m/s and 10 m/s are presented.

The same simulation environment is used in all simulations in subsequent sections. Other specific simulation parameters, or any modifications would be mentioned as needed. In order to improve the accuracy, 15 runs are performed for every case.

Link lifetime duration is calculated as the duration of continuous connection time between a node and its neighbor. In order to remove any edge effect, a link duration is considered only when the link is broken before the end of the simulation.

As an illustration, Figure 2 shows the plots for link lifetime distribution for the random waypoint model. Plots of lifetime distribution for other mobility models can be found in [23]. To remove the effects of short simulation time for low speeds (1 m/s), we conducted experiments for 9000 secs. We can see that both plots exhibit similar behavior: unimodal and positively skewed. The modal values of link durations is a significant property in these plots. The modal values tend to decrease with increase in speed. As the speed increases, the duration at which the 99 percentile value occurs also decreases. At a speed of 10 m/s, link durations above 500 secs are rare. Gerharz et al. [11] show in their link duration study that the histogram's peak (modal value) occurs roughly at the transit time of two mobile nodes crossing each other's transmission range. From our results we did not find this pattern in majority of the cases.

The collected link duration values are used to calculate the residual link lifetime. The residual lifetime value is computed as follows. Let  $l_i$  be the number of links with link duration  $i$  secs and  $R_a$  be the average residual link lifetime when the current link age is  $a$ .

$$R_a = \left( \sum_{i>a} (l_i * i) / \sum_{i>a} l_i \right) - a; \quad (1)$$

In other words, the residual lifetime for a link of age  $a$  is the average lifetime

of all links with durations above the age  $a$ , minus age  $a$ .

### 3.3 Associating Parametric Statistical Model for the Lifetime Data

The problem we consider can be described as follows. Suppose we have a random sample  $X_1, X_2, \dots, X_n$  of a parent random variable  $X$ , with distribution function  $F$ . Given that  $F$  is a member of one of a set of parametric families of distribution functions, say  $F_1, F_2, \dots, F_k$ , we have to decide which one of these  $k$  families best fits the sample.

#### 3.3.1 Choice of Lifetime Distribution Models

In the field of reliability engineering, the lifetime of entities are typically described using a “graphical representation” called *Bathtub Curve* [24], as shown in Figure 3. By definition, bathtub curve is a plot of instantaneous failure rates versus time, which is used to classify the failure rates. Bathtub curve describes the relative failure rate of an entire collection of entities over a period, and not just a single entity. A bathtub curve can be described as consisting of three sections: infant mortality failures, random failures, and wear-out failures.

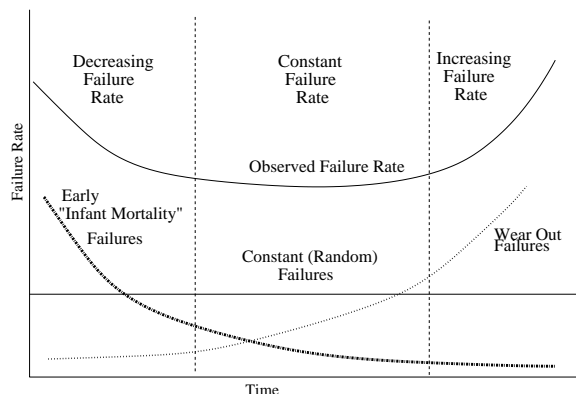


Fig. 3. Bathtub curve

Typical distribution models used for lifetimes are exponential, Weibull, log-normal and gamma [25]. The exponential distribution has a single parameter whereas other distributions have 2 parameters.

The probability density function of  $X$  having exponential distribution is given as:

$$f(x) = \lambda e^{-\lambda x}$$

The failure rate (also termed as Mean Time To Failure (MTTF)) reduces to the constant  $\lambda$  for any time. The exponential distribution is the only distribution to have a constant failure rate and is an excellent model for the second section (random failures, with constant failure rate) of the bathtub curve.

These type of failures are sometimes also referred to as “Intrinsic” failures. The exponential distribution has been used for link lifetime [7, 26] and path durations [6, 27].

The Weibull distribution is one of the most widely used lifetime distributions in reliability engineering. It is a very flexible lifetime distribution model with **two** parameters [28]. The probability density function of  $X$  having Weibull distribution is given as:

$$f(x) = \begin{cases} \frac{\beta}{\alpha} \left(\frac{t}{\alpha}\right)^\beta \exp^{-\left(\frac{t}{\alpha}\right)^\beta} & x > 0 \\ 0 & x \leq 0 \end{cases}$$

where  $\beta$  is called the shape parameter and is typically between 0.5 and 8, which determines the shape of the Weibull probability density function. For specified value of  $\beta$ , Weibull is identical to various one parameter distributions, including exponential and normal.  $\alpha$  is the scale parameter, and is also known as characteristic life (63.2 percent of the link population fails by the characteristic life point, regardless of the value of  $\beta$ ). Weibull can be used to model all three types of failure.

According to the central limit theorem (CLT), the probability distribution of a variable, that is the product of many independent random variables (none of which dominates the result) is lognormal [29]. Typically, lognormal distributions are generated by processes that follow the law of proportionate effect (multiplicative process) [30]. It is commonly used to model the lives of units whose failure modes are of a fatigue-stress nature.

The probability density function of  $X$  having lognormal distribution is given as:

$$f(x) = \begin{cases} \frac{1}{\sqrt{2\pi\sigma x}} \exp \left\{ -\frac{(\ln x - \mu)^2}{2\sigma^2} \right\} & x > 0 \\ 0 & x \leq 0 \end{cases}$$

Here  $x$  is the variate,  $\mu$  is the mean value of the log of the variate, and  $\sigma^2$  is the variance of the log of the variate.

For smaller values of  $\sigma$ , lognormal shapes are similar to Weibull shapes with larger  $\beta$ s, and for larger  $\sigma$  values, the curves are similar to Weibull shapes with smaller  $\beta$ s. Therefore, both the distributions are flexible and a careful decision should be made when choosing the one to use (especially for smaller samples). For larger samples, however, this difficulty on choice is reduced drastically [29].

Gamma is also one of the popular models used in system reliability studies. Similar to Weibull, Gamma can also be used to model in different applications, and for different type of failures. Gamma also includes exponential distribution as a special case, and also has monotonous failure rate (only lognormal exhibits

unimodal failure rate).

### 3.3.2 Selection of Model - Maximum Likelihood Analysis

In some circumstances, *physical considerations* alone can identify the appropriate family of distributions [15]. For example, when there is “no premium for waiting” and “lack of memory” property, the family of exponential distributions can be the ideal model. In practice, however, when such consideration is not available, a choice may be based upon mathematical analysis or on an understanding that a particular family is “rich” enough to include a good fit to the data [14].

The technique chosen is the maximum likelihood estimation, where for every alternative family under consideration it selects the family that yields the largest maximum likelihood. In our work, we use minimum Kolmogorov distance method [31], which is similar to maximum likelihood method. The additional process involved here is to determine the “Kolmogorov distance” between the specific candidate and the empirical distribution. The distribution that yields the minimum distance is chosen.

For the actual data processing, we used a curve-fitting software called Easy-Fit [32] which implements the minimum Kolmogorov distance method.

Table 1 provides a summary of the decision process derived from [15]. Given a data set and the maximum likelihood criteria, the most likely parent distribution is selected. Table 1 also provides the conditions whereby the decision can be made with high confidence.

In the following section, we will describe our initial findings based on the application of maximum likelihood analysis. Note that this is only the initial guess and additional confirmation based on degradation analysis and model analysis are needed.

### 3.3.3 Distribution Model for Random Waypoint

Using the data collected, the best fit distribution for random waypoint based on maximum likelihood method is lognormal distribution.

We know that the shape of the lognormal is affected by the values of both  $\mu$  (scale parameter) and  $\sigma^2$  (shape parameter). The density is more spread for higher values of  $\mu$ , whereas, it is more skewed (towards left) for higher values of  $\sigma^2$ . For low speed RWP, the parameters  $\mu$  and  $\sigma$  (considering lognormal) are 6.3757 and 0.8181. Whereas, for high speeds the parameters are 4.163 and 0.7253. A small (less than 1) shape parameter indicates a narrow range

Selection	Alternatives	Probability of Choosing Correctly
Lognormal	exponential	very high even for lesser samples
	weibull	exceeds 0.97 even for samples less than 100
	Gamma	very high for shape parameter greater than 0.25
Weibull	exponential	very high when shape parameter is greater than 1
	Lognormal	very high even for lesser samples, and independent of shape parameter
	Gamma	high only using minimum Kolmogorov distance technique, with larger sample size
Gamma	exponential	very high when shape parameter is greater than 1
	weibull	high only using minimum Kolmogorov distance technique, with larger sample size
	Lognormal	very high for shape parameter $> 1$ and minimum Kolmogorov distance technique

Table 1  
Selection of best-fit Distribution

of failure times and implies few early failures will occur. Also, large scale parameters implies a longer mean time to failure (MTTF) [25, 33].

From these parameters we can conclude that the failure rates follow the wear-out type of failure. For wear-out failures, the lifetimes are dependent on the current age, and the link wears out rather than experiencing a random break. From the plots for random waypoint, we can see that the lifetimes 0 - 400 secs (for low speeds) and 0 - 40 secs (for low speeds) are not the modal class. This also shows that the exponential distribution is a poor fit to the data collected.

From Table 1, we see that with lognormal data and with lognormal and Weibull as alternatives (or vice versa), the probability of choosing the correct distribution (using minimum Kolmogorov distance) is close to 1 with sample size greater than 100. Similarly, with shape parameter much larger than 0.25, Gamma distribution can be ruled out.

In summary, we conclude that with high probability the data generated by the experiments on random waypoint model is lognormal.

### 3.3.4 Distribution Model for RPGM

Considering Kolmogorov minimum distance technique, the best fit is Weibull for RPGM 2/3 low speed (1 m/s) and RPGM1(single group of 50 nodes) high speed (10 m/s). On the other hand, the best fit is again lognormal for high speeds RPGM2 and RPGM3. As the reasoning for selecting lognormal distribution has just been presented for RWP, we will present only the reasoning for picking Weibull.

For low speed RPGM 2/3 mobility models, the  $\beta$  (shape parameter) value is around 1.5 to 2.5. This parameter gives clue about the failure mechanism, since different slopes ( $\beta$ 's), imply different classes of failure modes. For Weibull distribution, if the shape parameter is less than 1, then the failure mode is infant mortality, if the parameter is equal to 1, it is random failure, and if it is greater than 1, the failure mode is wear-out [25, 33]. From the values of  $\beta$  obtained, we can conclude that the failures are purely wear-out failures.

We can also show that the best-fit model is Weibull by considering the alternatives. Based on the shape parameter, which is much larger than 1, we can exclude exponential distribution. Based on maximum likelihood criteria, lognormal is unlikely to be an alternative. Finally, for gamma, a large number of samples is needed, and this is available. Therefore, with high probability, the distributions chosen (Weibull for lower speeds RPGM and lognormal for higher speeds) is correct is very high (close to 1).

### 3.3.5 Manhattan and Campus Mobility

For Manhattan mobility scenarios, the best fit for both low and high speeds (1m/s and 10m/s) is Gamma distribution. The shape parameter for low speed was 1.6338 and for high speed was 1.8036.

For campus mobility, the best fit for both low and high speeds (1m/s and 10m/s) is Lognormal distribution, with shape parameters 1.54 and 1.40, respectively. The scale parameters are 4.08 and 4.22.

A summary of the findings for all the mobility models studied is presented in Table 2. *Across all mobility models studied, link exhibits wear-out failures rather than random or infant-mortality failures.*

## 3.4 Link Degradation Analysis

With the initial guess, the next task is to perform additional verification based on degradation analysis. In this work, the term degradation refers to how a

Distribution	PDF	Estimated Cases
Exponential	$\lambda e^{-\lambda x}$	
Lognormal	$\frac{1}{\sqrt{2\pi}\sigma x} \exp \left\{ -\frac{(\ln \frac{x-\mu}{\sigma})^2}{2\sigma^2} \right\}$	RWP, RPGM2/3 (HS) Campus
Weibull	$\frac{\beta}{\alpha} \left(\frac{x}{\alpha}\right)^{\beta} \exp^{-\left(\frac{x}{\alpha}\right)^{\beta}}$	RPGM1, RPGM2/3 (LS)
Gamma	$\frac{\beta^{\gamma}}{\Gamma(\gamma)} x^{\gamma-1} \exp^{-\beta x}$	Manhattan

Table 2

PDF of different distribution models with estimated best-fit cases. (HS) - High Speed, (LS) - Low Speed

node gradually moves out of another node's transmission range. Therefore, the degradation level is measured in terms of distance between the nodes.

We denote the degradation level, or true degradation path of a particular link, by  $D(t)$ ,  $t > 0$ . In simulations, values of  $D(t)$  are sampled at discrete points in time,  $(t_1, t_2, \dots)$ . Observed sample degradation path of link  $i$  at time  $t_j$  is

$$y_{ij} = D_{ij} + \epsilon_{ij}$$

where  $D_{ij}$  is the degradation path  $D(t_{ij})$  for unit  $i$  at time  $t$ .  $\epsilon_{ij}$  describe a combination of measurement and model error.

As an illustration of the degradation process, we show the result of an experiment using only 2 nodes, which are separated initially by 100 m. The area of the simulation is 1000 m x 1000 m, and other node parameters (like transmission range) remain the same. The nodes randomly pick a destination and speed (maximum speed of 10 m/s, same as random waypoint model) and move towards that destination with the chosen speed. Each simulation runs for 50 secs and is repeated for 1000 times.

The best-fit distribution for this degradation process is lognormal (using the minimum Kolmogorov distance technique). The fit-curve and the measurement data are shown in Figure 4 using bin size of 4s.

In the next step, we model the degradation process analytically to justify the associated distribution of the link lifetimes of the different mobility model. Due to space constraint, we will only outline the approach for showing that link lifetime under random waypoint mobility scenarios has lognormal behavior.

If  $T$  is a random variable describing the failure time of a link, then the failure

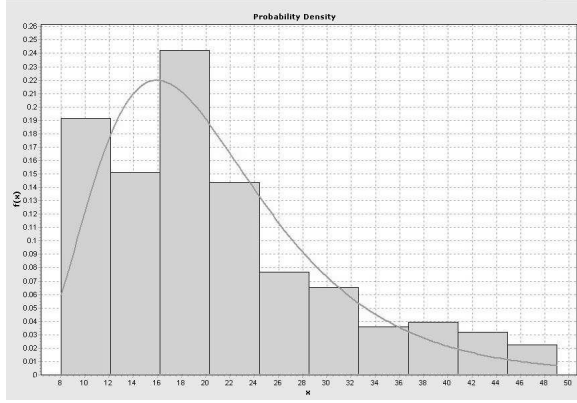


Fig. 4. PDF of lifetimes considering 2 nodes (probability distribution of failure time) can be written as:

$$Pr(T \leq t) = F(t) = Pr(D(t, \beta_1, \beta_2, \beta_n) \leq D_f)$$

$D_f$  is the threshold degradation level (which is 250 m in our experiment).

Variability causes links between nodes to fail at different times. A degradation model should account for the important sources of variability in a failure process. Considering the link degradation process, and the underlying reasons behind the link degradation, we can represent degradation path of a particular link as:

$$D(t) = \beta_1 + \beta_2 * t$$

$\beta_1$  is the initial amount of degradation, and in our previous experiment the value of  $\beta_1$  is fixed (100m). We know that the distance between two nodes, when nodes are moving, is largely dependent on the node speeds and directions. Therefore, we consider  $\beta_2$  to be the reciprocal of relative velocity. Further, we know that failure time is proportional to reciprocal of relative velocity times  $D_f - \beta_1$ . Let  $v(n, t)$  and  $\theta(n, t)$  be speed and direction of node  $n$  at time  $t$ , then magnitude of relative velocity is:  $RV(i, j, t) = \sqrt{a^2 + b^2}$ , where  $a = v(i, t)\cos\theta(i, t) - v(j, t)\cos\theta(j, t)$  and  $b = v(i, t)\sin\theta(i, t) - v(j, t)\sin\theta(j, t)$ .

Therefore,  $F(t)$  of link lifetime, in terms of  $D(t)$  the link degradation can be written as:

$$F(t; \beta_1, \beta_2) = Pr(D(t) > D_f) = Pr(\beta_2 > \frac{D_f - \beta_1}{t})$$

Now, to show that  $F(t)$  is log-normal we have to show that right hand side (RHS) is lognormal, or  $\beta_2$  has lognormal rate.

We measure the reciprocal of relative velocities between two nodes moving at random speeds and found that the data follows lognormal distribution using the Kolmogorov minimum distance technique.

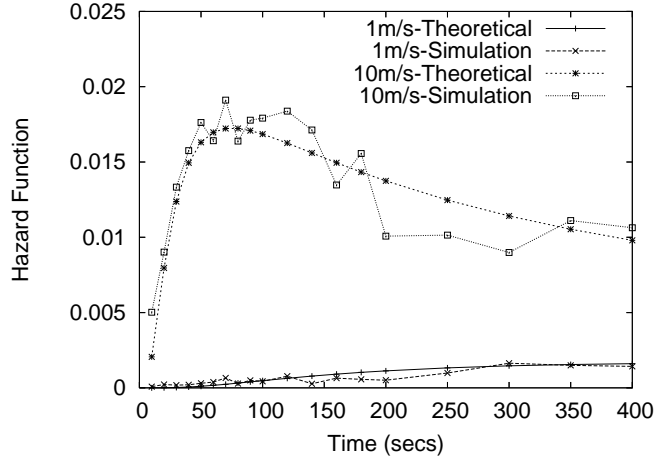


Fig. 5. Hazard function of random waypoint

### 3.5 Model Analysis

In the previous section, we collected the link lifetime data and associated a parametric statistical model to the data. The obvious question at this point will be: how good is the fit between the chosen distribution and the measured data? This issue is addressed in the final step as shown in Figure 1. Here, we assume that the model associated to the data is correct and try to predict the behavior.

In the context of reliability engineering, typically questions are of the following form. What is the probability that a link will sustain beyond some time  $t$ ? What is the probability that a link will break in the next instant, given that it has survived to the time  $t$ ? The answers to these questions are obtained by expressing the earlier distribution functions differently. Such different representations are hazard and survival functions.

We will illustrate how the analysis is performed using hazard function for the lifetime distribution model of random waypoint. The procedure for the other models is similar.

The hazard function (hazard rate, instantaneous failure rate) of the link is defined as the rate of change of the cumulative failure probability divided by the probability that the link will not already be failed by time  $t$  [29]. That is:

$$\lambda = \frac{dF(t)/dt}{1 - F(t)} = \frac{f(t)}{1 - F(t)}$$

The hazard function of a lognormal process is defined by [34]

$$\lambda(t) = \frac{\phi(d)}{t\sigma\Phi(-d)}$$

where  $d$  is given as  $\frac{\log_e t - \mu}{\sigma}$ ,  $\phi$  is the probability density function of the standard normal distribution and  $\Phi$  is the cumulative distribution function of the standard normal distribution.

Figure 5 shows the hazard function for random waypoint. It can be seen that the values for simulation and analysis match fairly well. The difference tends to be larger at larger values of time, at high speed, because there are less samples available.

The initial part of the hazard function is concave for higher speeds, indicating the increase in failure rate (at a decreasing rate) as the time increases. For lower speeds, the hazard function still increases with time, but the increase is less. After 100 secs, for higher speed, however, the hazard function decreases with respect to time (approaching to 0 as  $t \rightarrow \infty$ ). For higher speeds, such large durations are not of interest since few links last for periods longer than that. Lognormal model is thus adequate to represent lifetimes.

Hazard function, in addition to being an useful function for reliability calculations, provides the information needed for troubleshooting, or classifying failure types. Similar to lognormal distribution (random waypoint and high speed group mobility), we plotted out reliability and hazard functions for Weibull and Gamma distribution. We found that the change in reliability decreases slowly in the initial period and then decreases sharply as the characteristic life is approached.

### 3.6 Discussion

After completing the lifetime distribution study, it is useful to summarize the findings here.

- (1) Link failures of all models studied are of wear-out type. Random failure (modeled by exponential distribution) is not appropriate.
- (2) Lognormal is a good model for the mobility with sufficient amount of “randomness” and changes. That includes RWP, campus mobility and RPGM 2/3 moving at high speed (10m/s).
- (3) For mobility models with relative stable links, for example, RPGM1 and RPGM 2/3 moving at low speed (1m/s), Weibull is a good model.
- (4) Finally, for the Manhattan model, where the links lifetime among objects is highly dependent on the independent decision made at road junctions, Gamma distribution is a good (and natural) fit.

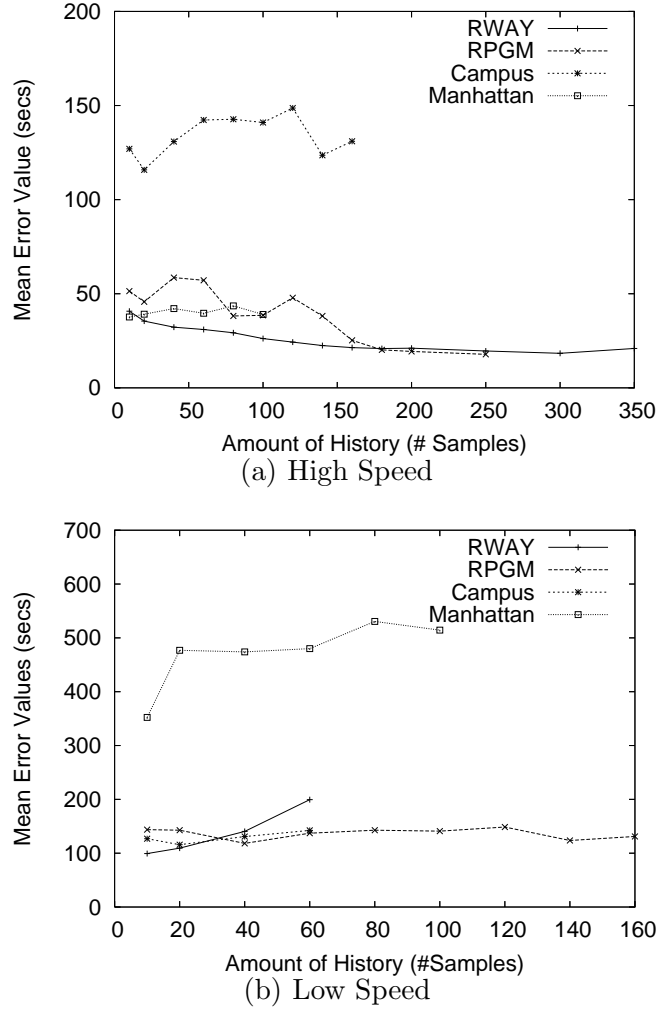


Fig. 6. Estimation error vs amount of history available

#### 4 Residual Lifetime Estimation

The basic approach to link lifetime estimation is for each node to maintain the history of link lifetimes of all neighboring nodes seen. By collecting this information and aggregating them into bins of say 10s, each node makes an estimate of the residual lifetime distribution using all the samples collected in equation (1) for all nodes. The approach is simple and the storage overhead of history maintenance is fixed since the number of bins is fixed.

A disadvantage with history based estimation approach is in deciding how much history is useful, as more history is not always better. For example, when the node mobility pattern changes, the estimation errors can be high since past history is no more relevant. Hence, the estimation process must be able to flush the history when necessary. The second and related problem is in the initialization phase when there is insufficient history. In these cases,

knowledge about link lifetime distribution would help to reduce the estimation error. We will discuss how our link lifetime estimation approach tries to address these issues.

In this section, we first present the residual link lifetime estimation process based on simple history values for all 4 mobility models. We also considered the additional cases of changes in mobility patterns. Finally, we show how availability of link lifetime distributions helps to reduce the estimation error.

#### *4.1 Estimation Errors for Various Mobility Models*

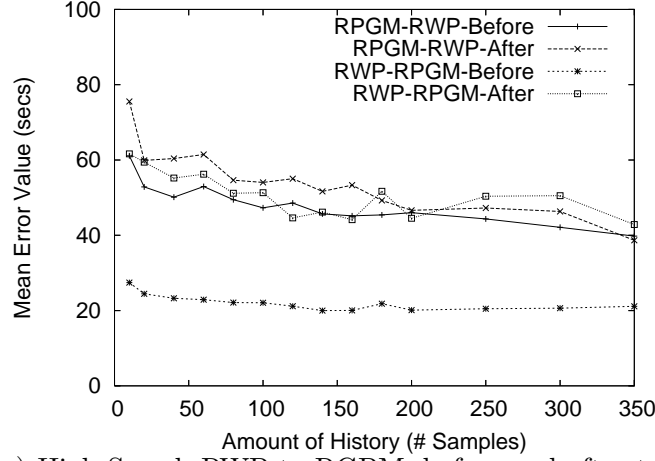
Figure 6 shows the estimation plots for all 4 mobility models at low and high speeds. The RPGM simulated is RPGM1. The y-axis shows the absolute value of the estimation error in seconds. The x-axis shows the amount of history data available, measured in number of samples available. The amount of history available depends on average node density and amount of link breakage observed. RWP tends to have the most history, while Campus and Manhattan have the least.

In general, speed has the largest impact on the amount of estimation errors. The errors are much larger for low speed than high speed. The difference is particularly large for Manhattan. The reason behind this difference in errors (for high speeds and low speeds) can be mainly attributed to the lack of history, when simulations are run for 1000 secs. Considering this lack of history, for low speeds, simulations were run for 9000 secs. This results in estimation errors (in secs) of larger durations. Whereas, this effect was not observed for high speeds. Overall, RWP has the smallest error with history based estimation, while campus and Manhattan tend to have much higher errors. For the campus model, this could be due to the presence of building structures and mobility, which depends on the user types.

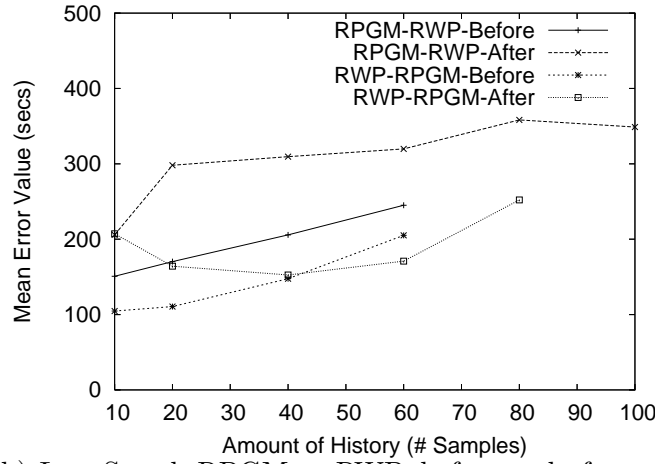
The results also clearly show that more history is not always better. For high speed RWP and RPGM1, estimation errors decrease steadily over time. However, for low speed RWP and Manhattan, estimation error increases over time with more history.

#### *4.2 Scenarios with Transitions between Random and Group Mobility*

In this section, we consider cases where the mobility patterns change from random waypoint to group mobility or vice versa. This transition occurs after 1000 secs of simulation period, where the total simulation period is for 2000 secs.



(a) High Speed, RWP to RGM, before and after transition



(b) Low Speed, RGM to RWP, before and after transition

Fig. 7. Amount of history Vs error with changes in mobility

Figure 7 shows the estimation errors for transition from RWP to RPGM1 and vice versa, for both low speed and high speed. The disadvantage of history based approach can be clearly seen in this case. After a change in mobility pattern, estimation error increases. For high speed RWP to RPGM1 transition, we can see that there is a large increase in the estimation errors after the transition. This is because, after the transition from random to group mobility the history contains more number of short link lifetimes compared to RPGM1. As a result, significant underestimation of link lifetime occurs. Further, after the transition, there will be fewer amount of new-samples of link lifetimes, as the nodes will follow group mobility. For the opposite case (RPGM1 to RWP transition), the increase in estimation errors (after transition) is not seen. This is because, after the transition from RPGM1 to RWP, the nodes tend to collect larger amount of new-samples of link lifetimes, and this helps in mitigating the estimation errors. In fact, the combined mean estimation error (for all

amount of samples combined), for transition from RPGM1 to RWP, is lesser for “after transition” compared to “before transition”. Similar effect can also be observed for the transition cases at low speed.

One technique to address this problem (increase in estimation errors when there are transitions from one mobility model to other) is to let a node detect the transition and reduces the amount of history kept so that the estimation errors can get reduced in a short period. There are a number of ways for a node to detect the transitions. In this work, we propose a technique where nodes maintain the information about its neighboring node densities. Neighbor densities give an indication of the mobility pattern. From simulations, we found that for RWP-to-RPGM and RPGM-to-RWP (for both high and low speeds) after transition, there is a change (either increase or decrease) in the node-density values. This shows that node-densities can be used to detect the transition. Unfortunately, the detection may not be straightforward for other combinations of mobility patterns.

### *4.3 Improving Estimation Process Using Distribution Information*

There are various ways in which we can exploit the link lifetime distribution information, including network reliability studies, estimating lifetimes and understanding of failure rates. In this section, we describe how we use the temporal properties study in preceding sections to improve the link lifetime estimation technique.

We illustrate our approach using the scenario when the mobility pattern changes. First, we utilize node-density measurements to detect the transitions from one mobility model to another mobility model (between RWP and RPGM or vice versa). Once a node estimates the transition, it gives up all the collected history, and starts collecting the lifetimes from stretch. In addition, knowledge of the associated statistical distribution is used to improve on link lifetime estimation. Note that estimation using distribution information is better because much fewer samples is needed than using historical values and the estimates will also be much more accurate.

To evaluate the improvement, we conducted a comparative study, considering the 2 mobility transition cases with the enhanced estimation procedure. For comparison, we look at 2 other approaches in which lifetimes are assumed to follow either a “uniform” or “exponential” distribution when there does not exist any history. We have seen that the uniform and the exponential distributions are not good-fit for either random or group mobility patterns but they provide convenient baseline comparison.

Figure 8 shows the mean estimation error values for all three approaches. The

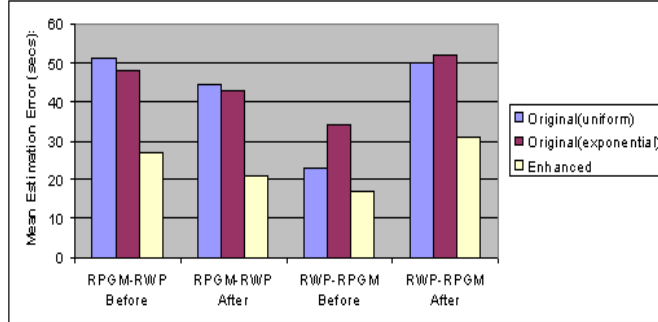


Fig. 8. Comparison with other distributions

approaches that use the uniform and exponential distribution are called *original (uniform)* and *original (exponential)*. Our approach is labeled *Enhanced*.

We can clearly see the improvements in both stages, before and after the transitions for both types of transitions. Compare to basing the estimation on either uniform or exponential distribution, use of the correct (Lognormal and Weibull) distributions reduces link lifetime estimation errors by 30% to 50% for RWP to RPGM and vice versa.

## 5 Application: Link lifetime aware packet scheduling

In this section, we describe the application of link lifetimes, where link lifetime is used as one of the packet scheduling parameters. Packet scheduling focuses on solving the problems associated with multiple sessions, within a single node, sharing the wireless link.

Our scheduling mechanism is termed as Channel aware Scheduling for Mobile Ad hoc networks (CaSMA). The term “channel-aware” in our work refers to having the knowledge of channel *conditions* or channel *state*. In CaSMA, *congestion state* and end-to-end *path lifetime* are used to represent channel conditions.

We use the term *path lifetime* (or path residual lifetime) to define the time interval for which the path associated for a flow is valid or exists. If the lifetime of each and every link of path  $\mathbf{P}$  from node  $i$  to node  $j$  is estimated as  $l_1, l_2, \dots, l_n$ , then the path lifetime  $P_{ij} = \min(l_1, l_2, \dots, l_n)$ . We use queue-size to represent the congestion state.

During the path setup, estimates of the path lifetimes are collected and stored. This path lifetime value is used as a parameter to represent the end-to-end channel condition. During packet scheduling, CaSMA selects the packets, which have high probability of reaching the destination, and takes into ac-

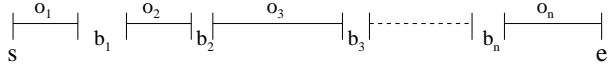


Fig. 9. Flow model

count the cost of a link break by giving priority to flows that have a longer normalized (with path residual lifetime) backlog queue. We show that CaSMA approximates an ideal scheduling mechanism in terms of maximizing the goodput and sharing the throughput (losses) fairly among the contending flows.

Our motivation for considering path residual lifetime and queue size can be understood by considering the impact of mobility on link lifetimes and the impact of link breakages. We found that the lifetime of the links can vary widely across different node-mobility speeds. That is, if there are  $n$  flows at any node, the lifetimes of those flows are unlikely to be similar and can vary over a large range. Hence, considering these lifetimes as a scheduling parameter can be useful, and can play a significant role in improving the performance. After link breakages, route re-establishment time can be in the order of milliseconds to tens of seconds. Further, the packets that are buffered by the nodes before any link breakage on the path can be lost, and may have to be retransmitted. Hence, it is also important to include the queue size on the scheduling decision.

In the succeeding section, we will describe the importance of link lifetimes by defining an ideal scheduler and explaining how CaSMA approximates the defined ideal scheduler.

### 5.1 Ideal Global Scheduler and Approximation

Before describing CaSMA in detail, we would first introduce the flow model considered and the optimizing parameters that we focus on in this part of the work.

#### 5.1.1 Flow Model and Optimizing parameters

Each request or flow  $i$  running through a path is described by a 6-tuple  $(T_i, C_i, s_i, e_i, \{o_i\}, \{b_i\})$ , where  $T_i$  is the minimum packet inter-arrival time,  $C_i$  is the maximum packet transmission time over a link,  $s_i$  and  $e_i$  are the start and termination period of a flow,  $\{o_i\}$  and  $\{b_i\}$  are the sets of continuous (duration for which the path exists or duration between link breakages) and breakpoint periods (duration for which path does not exist), respectively. We use  $o_i$  to represent single continuous period of flow  $i$ . The relation between  $s, e$  and  $o_i, b_i$  is as shown in Figure 9. If we focus only on the important flow parameters, we can reduce the flow representation from 6-tuple to 3-tuple:  $(T_i, C_i, o_i)$ . This is mainly because at any given time the scheduler is aware

Notation	Description
$o$	Continuous period
$n, m$	No. of flows
$r$	No. of packets existing in a queue
$X$	No. of packets served for a flow
$\alpha$	Proportion of $r$ of service received by a flow
$\zeta$	Schedulable set
$\Gamma$	Flow set
$T$	Minimum packet inter-arrival time
$C$	Maximum packet transmission time

Table 3  
Notations used

of a single continuous period value, and the other three parameters  $s, e, b_i$  are not available to the scheduler. Important notations used in the remaining part of this work is summarized in the Table 3, to make the reading easier.

The important optimizing factors of *CaSMA* are *merit* and *backlog* of a schedule. The merit  $M(H)$  of a schedule is based on the number of packets scheduled for transmission that successfully reaches its destination. Packets which do get transmitted for a few hops and get dropped at any of the intermediate nodes will not contribute for the merit of the schedule. The *backlog* is defined as the amount of packets of all the flows that remain in the network at the end of their respective continuous period.

Hence, the goal of *CaSMA* is to maximize the *merit* and minimize the *backlog*, distributed fairly across all the existing flows in the node, to reduce the delay and loss due to link breakages.

### 5.1.2 Global Ideal Scheduler

Let us consider a simple model with multiple flows over a single bottleneck link where we have a single scheduler. After the single shared link (with infinite lifetime), these flows use different (non-shared) links with different lifetime.

Let us assume a global scheduler -  $S_i$ , which schedules these flows (“m” flows). Let us consider a single continuous period  $o$  of “m” flows, with arrivals within this continuous period, and no further arrivals. That is, let us take a single snapshot in time of  $m$  flows with each flow having single continuous period of varying durations. For simplicity, let all flows have same  $T = 1$ , and  $C = 1$ . Therefore,  $S_i$  can schedule at most  $r_{max}$  packets in  $o_{max}$  period, where  $o_{max}$  is

the maximum continuous period of any flow (or total interval of the snapshot).  $r_i$  represents the number of packets existing for flow  $i$ .

We, however, know that maximum number of packets existing in all the queues is  $\sum_{i=1}^n r_i$ . Let us call this value as  $r_{sum}$ . Therefore, percentage ratio of throughput would be  $\frac{r_{max}}{r_{sum}}$ . Now, we adopt a fairness criterion, where this ratio is maintained across all the flows. In other words, the losses/backlog is proportionately distributed across all the flows. The idea here is that all sharers constrained by the same problem are treated fairly by assigning the proportionally equal throughputs. That is, for each flow  $i$ , the throughput it would receive is

$$r_i * \frac{r_{max}}{r_{sum}}$$

Further, losses at each queue would be

$$r_i \left(1 - \frac{r_{max}}{r_{sum}}\right)$$

The rationale behind having this formulation for an ideal scheduler is based on the argument that shorter continuous periods of flows are purely due to the inherent property of ad hoc networks. Therefore, we should not penalize flows which suffer due to the inherent property of the network. Further, the scheduler will not be aware of the amount of service a flow has received in the previous continuous period (if existed) or the amount of service a flow will receive in the next continuous period. Therefore, we go by the assumption that providing equal proportion of service in the current set of continuous periods should prove to be advantageous.

## 5.2 Design of CaSMA

CaSMA is designed to approximate the global scheduler through two features. First, through the design of parameters used to make packet-scheduling decisions. Second, by introducing the concept of schedulability condition. The parameters focus on minimizing the backlog, whereas the schedulability condition maximizes the merit of the scheduler.

### 5.2.1 Parameters used for scheduling decisions

In CaSMA, the parameters are chosen to achieve following two goals:

- provide higher priority to flows which take short-lived paths, and
- proportion of service received for each flow will remain similar.

*CaSMA* uses  $\frac{QS}{RLT}$ , where QS is queue size and RLT is the residual life time, and *eligible-service* as parameters to make scheduling decision. It can be shown easily that, serving queues which has higher  $\frac{QS}{RLT}$  values first will result in providing higher priority to flows which take short-lived paths. However, there are cases where short-lived flows can receive proportionately greater service. We avoid this by having an additional parameter termed as *eligible – service*, for each flow. This *eligible – service* for any flow  $i$  is equivalent to  $\frac{r_{max}}{r_{sum}}$ , and is computed by considering the  $r_i$ s, which is given as follows:

$$\frac{(r_i * \frac{C_i}{T_i})}{\sum_{j=1}^n r_j * \frac{C_j}{T_j}} * (r_{max} * \frac{C_{max}}{T_{max}})$$

$C_{max}$  and  $T_{max}$  indicates maximum possible  $C$  and  $T$ , respectively. The first term indicates the ratio of the work to be performed for a flow  $i$  and the total amount of work considering all flows. Whereas, the second term indicates the maximum work that can be done, and this term, in practice, is related to the maximum wireless link rate.

We update this parameter (*eligible – service*) only when new flows arrive or existing flows leave. The priority is given to flows considering both the request rate and eligible-service. Higher priority is given to flows whose request rate is high, and which has not yet received its eligible-service. This parameter will ensure that flows do not receive greater service (in proportion) at the cost of other flows.

It can be seen that the combination of these two parameters ( $\frac{QS}{RLT}$  and *eligible – service*) achieve the above mentioned two goals. The detailed description of the design of the parameters can be found in [35]

In the remaining part of this section, we will describe how we enhance the approximation of ideal scheduler by considering end-to-end packet scheduling.

### 5.2.2 Schedulability

A set of flows  $\Gamma$  is said to be “schedulable” ( $S$ ) if none of the flows has packets queued in the intermediate nodes at the end of their respective continuous periods. Any set of flows at a node that are schedulable over a link is termed as “schedulable set”.

A schedulable set (set of flows that are schedulable) is derived as follows. Let us assume that a node has  $n$  flows, of which it has to choose  $m$  flows to form a schedulable set. We use the classic result of real-time scheduling [36], and define the necessary condition for a set of flows to be schedulable over a link

is given as

$$\sum_{i=1}^m \left(\frac{C_i}{T_i}\right) \leq 1 \quad (2)$$

In addition, we know that there are different combinations that are possible in choosing  $m$  flows out of  $n$  flows ( $C_n^m$ ). We know that the value of  $m$  is dependent on the  $C_i$  and  $T_i$  values. For example, value of  $m$  becomes smaller for smaller values of  $T_i$ . Hence, we have to decide on a specific way to choose  $m$  flows out of  $n$  flows.

In our work, we choose the  $m$  flows considering the residual lifetime values of the flows. Scheduling based on residual lifetime is similar to earliest deadline scheduling (EDF). Therefore, based on the results from EDF scheduling [37] and adhering to the approach of choosing smallest residual lifetime first, we sort all the  $n$  flows in terms of the increasing residual lifetime, and from this sorted set we choose the first  $m$  flows. These  $m$  flows form our schedulable set  $\zeta$ .

Let us illustrate the process using an example. As shown in Figure 10. Let  $\{a, b, c, d\}$  be the flows at node ‘D’. Let  $\{2, 4, 4, 6\}$  and  $\{1/2, 1/4, 1/4, 1/6\}$  be their continuous periods and rates ( $\frac{C}{T}$ ), respectively. SCH indicates scheduler at a node. The scheduler at node ‘D’ chooses flows  $\{a, b, c\}$  as schedulable following the condition given by equation 2. Flows  $\{a, b, c\}$  are chosen considering their continuous periods and the rates. We can see that an addition of flow  $d$  will violate the condition, that is, summation of the rate values ( $\frac{C_i}{T_i}$ ) will be greater than 1.

We know that if a flow is schedulable at all the intermediate nodes, then it is schedulable over the path. The idea is analogous to the *series of traffic lights*. It is useful to turn the first light green when all the remaining lights will turn green within some acceptable duration. This technique helps in increasing the *merit* of a scheduler, as priorities are given to packets which will be “completely served”.

The notion of schedulability takes on only binary values (TRUE/FALSE). When we use this parameter in the algorithm, the mechanism just makes the decision for given values and existing conditions. This decision process is used to build the schedulable-list message, as described below, following the example in Figure 10.

Consider three nodes  $S$ ,  $I$ , and  $D$  as shown in Figure 10. We will focus on a single flow ‘a’ starting at node ‘S’, with intermediate node ‘I’ and terminating at node ‘D’. Let  $\{a, b, c, d\}$  be the flows at ‘D’. Let  $\{2, 4, 4, 6\}$  and  $\{1/2, 1/4, 1/4, 1/6\}$  be their continuous periods and rates ( $\frac{C}{T}$ ), respectively. Node ‘D’ chooses flows  $\{a, b, c\}$  as schedulable following the condition given by equation

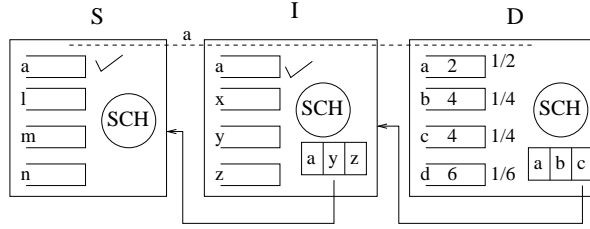


Fig. 10. Schedulability example

2, and creates a schedulability-list message (list of flows schedulable), which is transmitted to the upstream neighboring nodes. When ‘I’ receives this message, it marks flow ‘a’ as schedulable at downstream (sets the schedulability value to TRUE), and builds its own schedulable-list (let it be  $\{a, y, z\}$ ) and transmits it to its upstream neighbors. In this manner, the schedulable-list message flows upstream until it reaches source node ‘S’, which upon receiving will mark flow ‘a’ as schedulable (at downstream). If either the destination node or any of the intermediate nodes does not include flow ‘a’ in their schedulable list message, then the source node will not set flow ‘a’ as schedulable (at downstream).

### 5.3 Algorithm

A single queue is maintained for every destination of the flows that a node carries, i.e., different flows to the same destination are enqueued in the same queue. The Dynamic Source Routing (DSR) [38] is enhanced to implement schedulability-list technique. The algorithm is as shown in **Algorithm 1**.

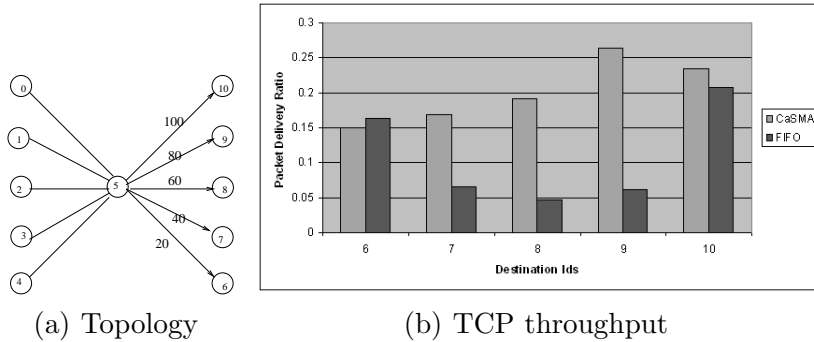


Fig. 11. Packet delivery ratio for different flows

### 5.4 Experimental Evaluation

In this section, we describe the experimental evaluation of CaSMA. In the first part of the simulation we consider a scenario where the scheduler has perfect knowledge of the link lifetimes. The goal is to provide the reader a

---

**Algorithm 1** Packet selection in CaSMA

---

**Require:** Initialize

- Per-destination queues are maintained,
- Each queue has [ queue size, residual life-time, eligible-service, schedulability, and throughput received ]

- 1: **repeat**
  - 2:   Consider a set of high-priority (real-time) queues
  - 3:   From this set of queues.
  - 4:   Select the set of queues, such that for every queue  $q$ ,  $q.schedulability = \text{TRUE}$
  - 5:   **if** No queue satisfies the condition ( $q.schedulability = \text{TRUE}$ ) **then**
  - 6:     Select all the queues.
  - 7:   **end if**
  - 8:   From these selected queues:
  - 9:   Select queue  $q$  such that the value  $\frac{QS(q)}{RLT(q)}$  is the maximum, and who have not yet received *eligible-service*
  - 10:   In case of tie select flow that has received least *throughput*
  - 11: **until** all queues are empty
- 

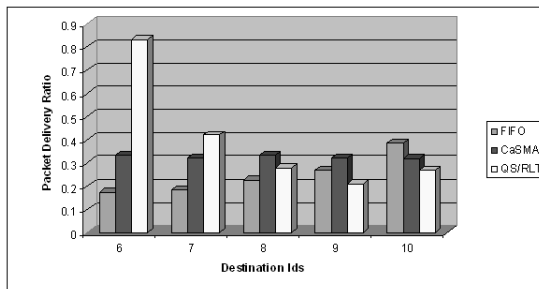


Fig. 12. Packet delivery ratio for different flows

better understanding of the advantages of CaSMA, when there are no lifetime estimation errors. In the second part of the simulation, we consider scenarios where link lifetime is estimated, and we compare the performance of various scheduling mechanisms. All our evaluations are carried out on NS-2 [19] simulator. Each mobile host has a transmission range of 250 m and shares a 2 Mbps radio channel with its neighbors. The simulation includes a two-ray ground reflection model and IEEE 802.11 MAC protocol.

#### 5.4.1 Performance Comparison with Known Path Lifetime

In this section, we focus on understanding the significance of the parameters considered ( $QS$ ,  $RLT$  and eligible-service). We considered a simple topology of 11 nodes, and simulation duration of 100 seconds. The topology is as shown in Figure 11(a). The source-destination pairs are  $[(0,6),(1,7),(2,8),(3,9),(4,10)]$ , with single intermediate node 5. In Figure 11(a), the numbers shown on links

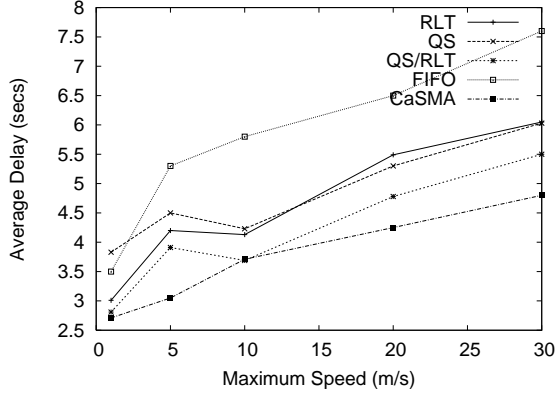


Fig. 13. Average delay versus maximum speed

between node 5 and {6, 7, 8, 9 and 10} indicate the respective link lifetimes.

We consider CBR flows transmitting at 400 kbps. The packet delivery ratios are shown in Figure 11(b). The delivery ratios for CaSMA are both even and higher compared to FIFO. For flow [0-6], FIFO has slightly better delivery ratio than CaSMA, but it performs badly for other flows. The delivery ratios are higher for CaSMA because CaSMA does not make an attempt to transfer those flows, whose link lifetime has expired. This shows that CaSMA is designed to provide service to the flows within their “lifetime” and not beyond that.

To focus on the importance of *eligible-service*, we slightly modified the source-destination pairs. Now, all the 5 flows initiate from node 5, flowing towards same destination, with same RLTs. The transmitting rate, however, is increased from 400 kbps to 600 kbps. Figure 12, shows the packet delivery ratios for FIFO, CaSMA and  $\frac{QS}{RLT}$  (without eligible-service). We can see that CaSMA, achieves both better packet delivery ratio and proportionate share. Though  $\frac{QS}{RLT}$  (without eligible-service) performs better than FIFO, the division of share is not fair ( flow [5-6] gets proportionately greater share). This is precisely the case for which eligible-service is included to handle, which results in providing fair share. It can also be seen that performance trend of FIFO and  $\frac{QS}{RLT}$  tend to be opposite. That is, FIFO’s performance increases with link lifetimes, whereas  $\frac{QS}{RLT}$ ’s performance decreases with link lifetime.

In summary, CaSMA is designed to perform such that flows with lesser residual lifetime get higher preference, and the losses (throughput) will remain proportionately same for all contending flows.

#### 5.4.2 Performance Comparison with Estimated Path Lifetime

In the second part of our simulation, we consider scenarios where lifetimes are estimated. We consider a network with 50 mobile nodes, with area 1000 m x

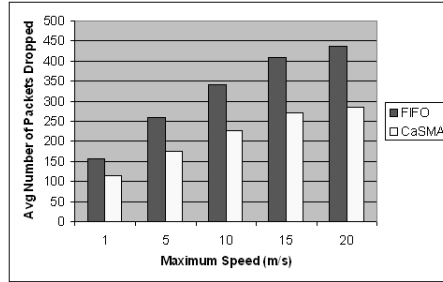


Fig. 14. Number of packets dropped at queue due to link breakage versus maximum node speed

1000 m. All the simulations are run for 1000 seconds, with 8 replications. In this part of evaluation, maximum speed of the node is varied from 1 m/s to 20 m/s.

The five mechanisms chosen are: FIFO (First In First Out), RLT (considering only residual life time), QS (considering only queue size), QS/RLT (considering both queue size and RLT), CaSMA (considering, queue size, RLT and schedulable-list).

For the first set of plots, we use 10 CBR flows with the transmission rate of 500 kbps. Figure 13 shows the plot of average delay values for all the five mechanisms. Considering the Figure 13, CaSMA performs best among all the schemes. This can be attributed to both the parameter chosen and the schedulable-list technique. Considering only the performance between QS/RLT and CaSMA, we can see the advantage of using schedulable-list technique.

To have a better understanding of the advantage we note the maximum and minimum of delay values, considering only FIFO and CaSMA. We found that the maximum values of CaSMA are also lesser compared to FIFO, whereas minimum values are almost the same. The main reason behind the reduction in delay values (average and maximum) is due to a reduction in the backlogs (or  $\gamma$  values, as described in preceding sections). The increase in backlogs can result in transmissions after a route-recovery delay. The backlog increase also has effect on the losses.

We also found that, with CaSMA the sharing of bandwidth is more fairer and better and had 25% less packet loss compared to FIFO. Figure 14 shows the number packets that are dropped at the queue due to link breakages (CaSMA in comparison with only FIFO). This parameter is directly related to the amount of backlog. From the figure, we can see that the backlogs using CaSMA is reduced by more than 30% - 40%. Further, we can see that increasing the frequency of topology changes, the amount of backlog also increases.

We further consider 10 TCP flows, and study the TCP performance in such scenarios. TCP flows are considered because, if the scheduler attempts to

schedule a packet whose path residual lifetime has expired, with high probability, it will result in dropping. This dropping will force TCP to reduce the congestion window, and in turn reduce the throughput. We studied the throughput performance of various schemes. We found that the TCP throughput for CaSMA increased in some cases up to 50% over FIFO. The reasons behind better TCP performance are the same as provided in the first part of this section.

In summary, we found that considering link lifetimes in packet-scheduling reduces the accumulation of packets (backlogs) at the end of flow on-times, and provide better end-to-end co-ordination and increases the merit of the scheduler.

## 6 Conclusion

This work emphasized the importance of having a accurate and thorough understanding of link lifetime behavior. We first carried out a detailed study of link lifetime distributions covering different mobility patterns. We found that link typically encounter wear-out failures, and lognormal and Weibull distributions prove to be a better fit.

As an application of the life estimation process, we described a novel packet scheduling mechanism CaSMA. CaSMA considers end-to-end channel condition represented as residual lifetime for channel-awareness, and also included a queue size parameter to make the scheduling scheme congestion-aware. This combination of parameters avoids the congestion and reduces the accumulation of packets (backlogs) at the end of route lifetimes.

## References

- [1] X. Perez-Costa, C. Bettstetter, and H. Hartenstein, "Toward a mobility metric for comparable & reproducible results in ad hoc networks research," *SIGMOBILE Mobile Computing and Communication Review*, vol. 7, no. 4, pp. 58–60, 2003.
- [2] F. Bai, N. Sadagopan, and A. Helmy, "IMPORTANT: A framework to systematically analyze the impact of mobility on performance of routing protocols for adhoc networks," in *Proceedings of The Conference on Computer Communications, Twenty-Second Annual Joint Conference of the IEEE Computer and Communications Societies(INFOCOM) 2003*, San Francisco, California, April 2003, pp. 825–835.

- [3] S. Cho and J. P. Hayes, "Impact of mobility on connection stability in ad hoc networks." in *Proceedings of IEEE Wireless Communications & Networking Conference (WCNC) 2005*, vol. 3, New Orleans, Louisiana, March 2005, pp. 1650–1656.
- [4] V. Lenders, J. Wagner, and M. May, "Measurements from an 802.11b mobile ad hoc network," in *Proceedings of IEEE International Symposium on a World of Wireless, Mobile and Multimedia Networks (WoWMoM) 2006*, Buffalo, New York, June 2006, pp. 519–524.
- [5] J. Tsumochi, K. Masayama, H. Uehara, and M. Yokoyama, "Impact of mobility metric on routing protocols for mobile ad hoc networks," in *Proceedings of Pacific Rim Conference on Communications*. Taipei, Taiwan: IEEE, 2003, pp. 1000 – 1003.
- [6] Y. Han, R. J. La, A. M. Makowski, and S. Lee, "Distribution of path durations in mobile ad-hoc networks: Palm's theorem to the rescue," *Computer Networks*, vol. 50, no. 12, pp. 1887–1900, 2006.
- [7] S. Arbindi, K. Namuduri, and R. Pendse, "Statistical estimation of route expiry times in on-demand ad hoc routing protocols," in *Proceedings of Second IEEE International Conference on Mobile Ad-hoc and Sensor Systems (MASS) 2005*, Washington, DC, November 2005, pp. 467– 471.
- [8] D. Turgut, S. K. Das, and M. Chatterjee, "Longevity of routes in mobile ad hoc networks." in *Proceedings of IEEE Vehicular Technology Conference (VTC) Spring 2001*, Rhodes, Greece, 2001, pp. 2833–2837.
- [9] Y.-C. Tseng, Y.-F. Li, and Y.-C. Chang, "On route lifetime in multihop mobile ad hoc networks," *IEEE Transactions on Mobile Computing*, vol. 2, no. 4, pp. 366–376, October 2003.
- [10] I. Gruber and H. Li, "Link expiration times in mobile ad hoc networks," in *Proceedings of IEEE Conference on Local Computer Networks (LCN) 2002*, Tampa, Florida, November 2002, pp. 743–750.
- [11] M. Gerharz, C. de Waal, M. Frank, and P. Martini, "Link stability in mobile wireless ad hoc networks," in *Proceedings of IEEE Conference on Local Computer Networks (LCN) 2002*, Tampa, Florida, November 2002, pp. 30–42.
- [12] Z. Cheng and W. B. Heinzelman, "Exploring long lifetime routing LLR in ad hoc networks," in *Proceedings of ACM International Workshop on Modeling Analysis and Simulation of Wireless and Mobile Systems (MSWiM) 2004*, Venice, Italy, October 2004, pp. 203–210.
- [13] Y.-C. Hu and D. B. Johnson, "Caching strategies in on-demand routing protocols for wireless ad hoc networks," in *Proceedings of ACM Annual International Conference on Mobile Computing and Networking (MOBICOM) 2000*, Boston, Massachusetts, August 2000, pp. 231–242.
- [14] J. L. Stanford and S. B. Vardeman, *Statistical methods for physical science*. Methods of experimental physics, San Diego CA: Academic Press, 1994.

- [15] A. W. Marshall, J. C. Meza, and I. Olkin, “Can data recognize its parent distribution?” *Journal of Computational and Graphical Statistics*, vol. 10, no. 3, pp. 555–582, September 2001.
- [16] T. Camp, J. Boleng, and V. Davies, “A survey of mobility models for ad hoc network research,” *Wireless Communications and Mobile Computing*, vol. 2, no. 5, pp. 483–502, 2002.
- [17] K. N. Sridhar, S. Hao, M. C. Chan, and A. L. Ananda, “Egress: Environment for generating realistic scenarios for simulations,” in *Proceedings of The 10-th IEEE/ACM International Symposium on Distributed Simulation and Real Time Applications*, 2006, pp. 15–24.
- [18] “EGRESS: Environment for generating realistic scenarios for simulations,” Available from <http://www.comp.nus.edu.sg/~sridhark/mantra/EGRESS.tar.gz>.
- [19] F. K. and V. K., “NS notes and documentation,” The VINT Project, UC Berkely, LBL, USC/ISI, and Xerox PARC, Available from <http://http://www.isi.edu/nsnam/vint/>, 1997.
- [20] “Toilers,” Available from <http://toilers.mines.edu>.
- [21] “Bonnmotion,” Available from <http://web.informatik.uni-bonn.de/IV/mitarbeiter/dewaal/bonnmotion/>.
- [22] “Important,” Available from <http://nile.usc.edu/important/>.
- [23] K. N. Sridhar and M. C. Chan, “Stability and hop-count based approach for route computation in MANET,” in *Proceedings of IEEE International Conference on Computer Communications and Networks (ICCCN) 2005*, San Diego, California, October 2005, pp. 25–31.
- [24] “Bathtub curve image,” Available from [http://commons.wikimedia.org/wiki/Image\;Bathtub\\\_curve.jpg](http://commons.wikimedia.org/wiki/Image\;Bathtub\_curve.jpg).
- [25] W. Q. Meeker and L. A. Escobar, *Statistical Methods for Reliability Data*. NY, New York: John Wiley & Sons, Inc, 1998.
- [26] J. Shengming, H. Dajiang, and R. Jianqiang, “A prediction-based link availability estimation for mobile ad hoc networks,” in *Proceedings of The Conference on Computer Communications, Twentieth Annual Joint Conference of the IEEE Computer and Communications Societies(INFOCOM) 2001*, Anchorage, Alaska, April 2001, pp. 1745–1752.
- [27] N. Sadagopan, F. Bai, B. Krishnamachari, and A. Helmy, “PATHS: analysis of path duration statistics and their impact on reactive MANET routing protocols,” in *Proceedings of ACM International Symposium on Mobile Ad Hoc Networking and Computing (MOBIHOC) 2003*, Annapolis, Maryland, June 2003, pp. 245–256.
- [28] W. Waloddi, “A statistical distribution function of wide applicability,” *Journal of Applied Mechanics*, vol. 18, pp. 293–297, 1951.

- [29] E. L. Crow and K. Shimizu, *Lognormal Distributions Theory and Applications*. NY, New York: Drekker, 1988.
- [30] J. Aitchison and J. Brown, *The Lognormal Distribution*. Cambridge, UK: Cambridge University Press, 1957.
- [31] C. A. Drossos and A. N. Philippou, “A note on minimum distance estimates,” *Annals of the Institute of Statistical Mathematics*, vol. 32, no. 1, pp. 121–123, December 1980.
- [32] “Easyfit 3.0,” MathWave Technologies, Available from <http://mathwave.com/downloads.html>, 2005.
- [33] C. Quesenberry and J. Kent, “Selecting among probability distributions used in reliability,” *American Statistical Association, Technometrics*, vol. 24, no. 1, pp. 59–65, February 1982.
- [34] “e-Handbook of statistical methods,” <http://www.itl.nist.gov/div898/handbook/>, Retrieved August 2006.
- [35] K. N. Sridhar and M. C. Chan, “Channel aware packet scheduling for mobile ad hoc networks,” in *Proceedings of IEEE International Symposium on a World of Wireless, Mobile and Multimedia Networks (WoWMoM) 2008*, Newport Beach, California, June 2008.
- [36] J. P. Lehoczky, L. Sha, and Y. Ding, “The rate monotonic scheduling algorithm: Exact characterization and average case behavior,” in *Proceedings of the Tenth IEEE Real-Time Systems Symposium*, IEEE. Santa Monica, California: Computer Society Press, Dec 1989, pp. 166–171.
- [37] C. L. Liu and J. W. Layland, “Scheduling algorithms for multiprogramming in a hard-real-time environment,” *Journal of ACM (JACM)*, vol. 20, no. 1, pp. 46–61, 1973.
- [38] D. B. Johnson, D. A. Maltz, and J. Broch, “DSR: the dynamic source routing protocol for multihop wireless ad hoc networks,” *Ad hoc networking Boston, MA: Addison-Wesley Longman Publishing Co., Inc.*, pp. 139–172, 2001.